CENTRAL LIBRARY
Indian Institute of Technology
KANPUR Thesis
Class No. 669.3
R18t

THERMAL BEHAVIOUR
OF
[illegible] FAULTS IN COPPER

A Thesis submitted in partial fulfilment

of the requirements for the

Degree of

MASTER OF TECHNOLOGY

in

Metallurgical Engineering

By

Gutti Varaprasada Rao

ME-1968-M-RAO-THE

To

THE DEPARTMENT OF METALLURGICAL ENGINEERING
INDIAN INSTITUTE OF TECHNOLOGY, KANPUR

December, 1968

Thesis
669.2
K18t

CERTIFICATE

Certified that the work presented in this Thesis has been carried out by G. Varaprasada Rao under our supervision and has not been submitted elsewhere for a Degree.

G.S Murty

Dr. M.N. Shetty
Asstt. Professor,
Dept. of Met. Engg.,
IIT/Kanpur

Dr. G.S. Murty
Asstt. Professor,
Dept. of Met. Engg.,
IIT/Kanpur

The author is indebted to Dr. M.N. Shetty for suggesting the problem and for aid and advice given during the course of investigation. He also wishes to thank Dr. G.S. Murty for the encouragement and many helpful discussions.

C O N T E N T S.

===

A B S T R A C T.

In order to obtain information about the thermal behaviour of stacking faults in f.c.c. metals, investigation was carried out on 99.999% purity copper using x-ray diffraction technique.

Patterson's theory was used to relate the shift in peak positions to the stacking fault probability. Making suitable approximations regarding dislocation density, it was possible to work out the variation of the fractional parameter ($\gamma_T / \gamma_{R.T}$) with temperature, in the temperature range 300° K. to 727° K. being the stacking fault energy at T° K. and , the one at room temperature.

The error introduced due to the thermal dependence of elastic constant and lattice parameter was eliminated.

Stacking fault energy was found to be linearly decreasing with temperature, the law of variation being $\gamma_T / \gamma_{RT} = 1.2377 - 0.0008277$.

==

LIST OF FIGURES.

--:--

INTRODUCTION

The crystals of face-centred cubic (f.c.c.) metals are made up of layers of atoms in a close packed arrangement, constituting the {111} planes of the lattice.

Normal to these layers, the sequence of stacking follows a three fold pattern that may be represented by the letter sequence... ..ABCABC....

In general, any perturbation in the perfect stacking order can be regarded as a stacking fault. Accordingly a stacking fault can be defined as the planar surface of separation between two regions of a crystal which have same orientation, but do not form a continuous lattice.

There are three types of faults that are possible in a face-centered cubic structure which are known as growth (or twin), deformation (or intrinsic), and extrinsic stacking faults.

A fault in the stacking sequence occuring in such a manner that the local pattern normal to the slip plane becomes ....ABCA$\bar{C}$ABC.... the stacking pattern being the same throughout the crystal except at the plane of the fault is designated as intrisic stacking fault.[1]

A second perturbation in the perfect {111} stacking order can occur leading to the sequence ....ABCA$\bar{C}$B$\bar{C}$ABC ...., and in this case the portions of the crystal in which the stacking pattern is the same are separated by an extraneous layer. This fault is designated as "extrinsic."

Further, twin or growth faults are found having the sequence of stacking....ABCA CBACB ...., a mirror plane or symmetry being present.

Of these it appears, deformation stacking faults are of greatest importance in the plastic deformation of metals and alloys. The intrisic stacking faults are of direct interest for the present study.

The principal lattice vectors, and therefore the most likely Burger's vectors for dislocations in the f.c.c. structure are of the type $\frac{a}{2}\langle 110\rangle$ and $a\langle 001\rangle$.

Since the energy of a $a[001]$ dislocation is double that of the energy of $\frac{a}{2}[110]$ dislocation, the dislocation of the former type are much less favoured energetically and in fact have not been observed. Fig. (1a) represents an $\frac{a}{2}[110]$ edge-dislocation in an f.c.c. lattice. The "extra half plane" consists of two (110) planes which occur in an ....ABAB .... sequence. Movement of this unit dislocation by glide involves a successive displacement such that the unit A + B configuration is retained. An unit dislocation lying on the close packed planes can lower its energy by dissociating into the imperfect dislocation as predicted by Heidenreich and Shockley[2]. Considering the process of slip on the (111) plane Fig. (2) and Fig. (3), the vector $\vec{b}_1$ ($= \frac{1}{2}$ a $[10\bar{1}]$) defines one of the observed slip directions. However, as pointed out by Thompson and Millington[3] consideration of atoms as regid balls restricts the slip movement in a zig zag path of the type B $\longrightarrow$ C $\longrightarrow$ B, following the vectors $\vec{b}_2$ ($= \frac{1}{6}$ a $[2\bar{1}1]$) and $\vec{b}_3$ ($= \frac{1}{6}$ a $[11\bar{2}]$) alternately. This process of slip with displacement of atom B to C alters the stacking sequence of (111) layers in the crystal.

In the edge dislocation in an f.c.c. lattice shown in Fig. (1a), the two planes consisting the inserted plane are separated by half a lattice vector. The elastic strain energy of such a complete dislocation can be reduced if these two inserted planes are separated from each other as shown in Fig.(1b). The edge of these two planes now forms a partial dislocation (the fact that the partial dislocations are not of pure edge character has been neglected in the figure for simplicity). The dissociation of complete Burgers vector $\vec{b}_c$ into partials ($\vec{b}_{pa}$, $\vec{b}_{pb}$) can be represented by the reaction of the type

$$\frac{a}{2}\ [110] = \frac{a}{6}\ [211] + \frac{a}{6}\ [12\bar{1}]$$

which is energetically favoured, the energy being reduced from $a^2/2$ to $a^2/3$. As these shockly partials separate out, a sheet of stacking fault is formed in the slip plane between them and the energy of this fault prevents them from separating too far.

When the distance 'η' between them exceeds a few atom spacings, the total energy of the fault is proportional to its area. Thus, if the energy per unit area of the fault is 'γ', the force per unit length exerted on the dislocations by the fault is also 'γ'. The partials repel each other elastically, the force of repulsion 'F' being approximately given by,

$$F = \gamma = \frac{\mu\,(\vec{b}_{Pa} \cdot \vec{b}_{Pb})}{2\pi\eta} = \frac{\mu a^2}{24\pi\eta} \qquad \ldots\ldots\ldots(1)$$

where 'μ' is the shear modulus and 'a' is the lattice parameter. Although in a deformed crystal the individual pairs of partial

dislocations are not necessarily in equilibrium, the internal stresses exerted by the dislocations acting on one another will increase the separation of some while decreasing that of others. A simple calculation indicates that for a crystal free from external stress, the mean stress tending to change the partials - separation - distance is zero.

Stacking faults can exert an important influence on the structural and mechanical properties of face centered cubic metals and alloys. Recrystallization[4,5], texture formation[6,7] and microstructure[8] can be related to the stacking fault energy of the material. Work hardening [8,9,10,11], as well as low temperature creep theories[12] also predict a relationship between cross slip and stacking fault energy.

There are many methods both direct and indirect, for determining the stacking fault energy. The direct methods employ the transmission electron-microscopy techniques to observe stacking faults. Indiret methods which are based on the microscopic effects of stacking faults, include measurements from X-ray diffraction lines, temperature dependence of stress-strain curves, incremental creep method, tilt boundary and twin boundary methods. The direct methods are superior since they deal with only the individual defects. One such direct method is the following.

Extended nodes and contracted nodes are observed in the network of dislocations lying on the (111) planes. Each of the three unit dislocation lines which joins such a node is split into

two shockley partials whose Burger's vectors are common to the other two split unit dislocations in the node, one to each. When the common partials of two split unit dislocations lie on the same side of the node, an extended node is formed; when they lie on opposite sides, the node is contracted. The stacking fault energy can be evaluated by measuring the radius of curvature 'R' and the inscribed radius 'ω' of the extended nodes.

Whelans[13] simplest model predicts the relation $\gamma = \frac{\mu b^2}{2R}$ There has been several modifications to this formula to take into account the character of the dislocations (Howie and Swann) and the variation of the line tension with the node character (Tholen and Siems) as well as the interaction of the partials. For actual analysis of the situation one may consult the reference. There can be errors introduced in the measurement in this method mainly due to the inaccuracy in the measurement of node radii and ambiguous assignment of the node character.

The limitation on this method arises because the nodes are visibly extended only for relatively low stacking fault energies, the upper limit being $\frac{\gamma_{max}}{\mu b} \simeq 10^{-2}$. This technique can be successfully applied only over a small range of values of 'γ'. If the stacking fault energy is too high, the resolving power of the microscope is too low to permit a sufficiently accurate measurement of the radii of curvature of dislocation nodes. If 'γ' is too low, the nodes cannot be isolated because of extensive faulting.

Among the indirect methods, X-ray diffraction technique is widely used to determine the stacking fault energy of metals. The earlier X-ray studies of faulted metals were based on measurement of X-ray peak breadths. Recent studies proved that the really important and interesting features of the diffraction patterns are second order features, such as the precise peakshape, small peak displacements and slight asymmetries, which are completely missed by working only with peak breadths.

Deformation faults produce a shift of the position of the peak[15], whereas twin faults cause the line profile to become asymmetric[16] and hence a shift in the centre of gravity. In addition to the broadening due to faulting, the peaks of cold worked f.c.c. metals are broadened by a reduction in the size of coherently diffracting domains as well as by the distortion within each domain[16]. The asymmetry may also be produced by the segregation of solutes at the stacking faults[17] in case of alloys and this will be very small if the scattering powers of solute and solvent atoms are similar. Warren and Averbeach's[18] method of Fourier analysis of line shapes provides information concerning the effective particle size 'De' the root mean square strain components $\langle \epsilon_L^2 \rangle^{\frac{1}{2}}$ and the compound fault probability $(1.5\alpha + \beta)$ where α and β stand for stacking fault probability and twin fault probability respectively. Patterson's theory[19] of the effect of stacking faults in f.c.c. materials on Bragg condition for diffraction relates the fault probability 'α'* to a shift in the Bragg

* 'α', the stacking fault probability is defined as the fraction of the whole surface of the close packed planes occupied by the faults.

X-ray diffraction peak position 'θ' between faulted and fault-free samples. Only the essential results of the theory that are useful in the present formulation will be given here, a detailed analysis of the theory being given in the Appendix.

According to the theory, the averaged value of peak shift is given by

$$\langle \Delta(2\theta^{\circ}) \rangle_{hkl} = \langle G_{at} \rangle j . \tan\theta_{o} . \alpha \qquad \ldots\ldots\ldots(3)$$

where j is the fraction of the (hkl) planes effected by stacking faults,

$G = \pm 90 \sqrt{3}\, h_3 / \pi^2 \ell_o^2$

'θ' is Bragg angle, and $\ell_0^2 = h^2 + k^2 + l^2$, hkl being the cubic indices.

The assumptions involved in the Patterson theory (such as the restriction of stacking faults to (111) planes only and a random distribution of them) have been examined previously in detail by several workers[20] and have been found to be generally valid.

Individual X-ray diffraction observations particularly those made with a diffractometer may be subject to considerable instrumental error such as that due to the non-coincidence of the surface of the plane of the specimen with the axis of the diffractometer. For this reason it is preferable to use the relative shift of the peaks of a pair of diffraction lines rather than to attempt to measure the shift of a single line as one changes from a faulted specimen to a fault-free specimen.

Considering the relative shift of (hkl) and (h'k'l') reflections and using equation (3), we have the lelation,

$$(2\theta_{hkl} - 2\theta_{h'k'l'})_{faulted} - (2\theta_{hkl} - 2\theta_{h'k'l'})_{fault\ free} = \left[(\langle G\rangle j \tan\theta)_{hkl} - (\langle G\rangle j \tan\theta)_{h'k'l'}\right] \alpha \quad \ldots\ldots(4)$$

If the faults are introduced by cold work as suggested by Barret[21] then the peak shift between annealed and cold worked sample is related to the stacking fault probability as,

$$(2\theta_{hkl} - 2\theta_{h'k'l'})_{CW} - (2\theta_{hkl} - 2\theta_{h'k'l'})_{An} = H \cdot \alpha \quad \ldots\ldots(5)$$

where
$$H = (\langle G\rangle j \tan\theta)_{hkl} - (\langle G\rangle j \tan\theta)_{h'k'l'} \quad \ldots\ldots(6)$$
or
$$\Delta\Delta 2\theta = H\alpha$$

The parameter H is a function of the indices of the planes alone and varies only slightly with composition (in case of alloys) or temperature. The values of $\langle G \rangle$ and j are tabulated for various planes by Wagner[22].

If 'ρ' is the dislocation density in the faulted sample, η ribbn width between two partials, and 'd' the interplanar spacing, then it can be seen that the stacking fault probability 'α' which is the fraction of slip planes that are faulted will be equal to:

$$\alpha = \eta \rho d \quad \ldots\ldots(7)$$

Using equations (1) and (7), th stacking fault probability can he related to the stacking fault energy:

$$\alpha = \rho d \left[\frac{\mu a^2}{24\pi\gamma}\right]$$

In a strict sense the stacking fault energy can be obtained only from the simultaneous measurements of stacking fault probability and dislocation density. In the absence of suitable techniques for the measurement of 'ρ' in the sample (as in the case of cold worked filings), by making suitable approximations concerning dislocation density, relative values of 'γ' may be obtained from the values of 'α' worked out from peak shift measurements.

Extensive studies on the occurence of stacking faults in binary alloys based on the solvent metals copper, silver and gold have been made using X-ray technique during the recent years[22, 24, 25,26] and in all these investigations pronounced increase of the degree of faulting with increasing solute content has been observed across the primary solid solution range. It has been also noticed that the dependence of stacking fault parameter 'α' with solute concentration is either linear or roughly parabolic and the variation of 'α' with composition is determined by certain factors[1,2]. In all these works, the stacking fault parameter at any composition is obtained from the relative peak shift between two reflections as one passes from cold worked sample (270 mesh product obtained from filing) to an annealed one. At any composition part of the sieved filings are used as cold worked sample in a 'as filed' condition and the other part of filings are given annealing treatment to form the annealed sample. The variation of dislocation density (introduced due to filing) with

composition has been neglected on the assumption that if the mechanism of filing were to be by pile up of dislocations, the dislocation density would be independent of shear modulus.

Measurements by Wagner[22] on Aluminium, filed under liquid nitrogen and measured at -160°C showed no trace of peakshift. Aluminium is evidently an extreme example in which there are no stacking faults. Christian and Spreadborough[27] measured a set of Ni-Co alloys, and found a deformation probability which was extremely small for Ni but increased rapidly with increasing 'Co' content. Warren and Ware Kois[28] made measurements on α-brass filed at room temperature, and found deformation fault probabilities which increased with zinc content reaching a value of $\alpha = 0.039$ at 35 percent Zn. These earlier investigations suggested that the stacking fault probability 'α' increases rapidly with increasing solute content, the variation of 'α' with composition is primarily defined by the electron/atom ratio, but that for a fixed electron/atom ratio, 'α' increases as the solute valency increases and the increase of ' ' is either linear or roughly parabolic.

Though many experimental and theoretical papers have delt with stacking faults, very little is yet known about the factors influencing the stacking fault-energy. Temperature is one of such factors, and a knowledge of temperature dependence of SFE is essential for a better understanding of material properties dependent on stacking fault energy.

Unfortunately, most of the available techniques are not suitable for thermal behaviour measurement to a sufficient accuracy. There are very few attempts made in this direction. Swann and Nutting[29] made an attempt to measure the stacking fault energy of copper -7% aluminium alloy as a function of temperature. They could not detect any appreciable change in radius of curvature of extended nodes upto 275°C but at 340°C a sharp increase in the stacking fault energy was apparantly observed. However, on cooling down the node did not expand again which was attributed to an apparent irreversible change. It has been observed that the stacking fault energy of silver decreases as the temperature is increased[30,31]. The observation was first made indirectly from measurements of critical shear stress at the onset of stage III hardening in bulk silver. The results were reported for temperature ranging from 170°C to 880°K. The essential result was also inferred directly from the measurements of radii of extended nodes in silver foils thinned from bulk Schwab[31] investigated the thermal behaviour of stacking faults in Graphite platelets by direct measurement and found that the essential temperature dependence of 'γ' in graphite is of the same order as that of 'k', the elastic coefficient.

It is of interest to extend the study to the temperature dependence of stacking fault energy.

Klein[32] discussed the complications involved in employing a heavily deformed metal for the measurement of thermal behaviour of

stacking faults, by X-ray technique. If the dislocation density could be approximated from the mean square strain $\langle \epsilon^2 \rangle$, determined by analysis of X-ray peak profiles, then relation (7) becomes $\gamma = A \left[\alpha/\epsilon^2\right]^{-1}$, 'A' being a constant. The unusual extent of variation of stacking fault energy (by a factor of 4 within a temperature range of 200°C in case of Cu-Zn alloys and by about a factor of 2 within a temperature range of 100°C in case of Au - Ag alloys) with annealing temperature suggests that the valid constant 'A' is dislocation configuration dependent parameter and is dependent on the annealing cycle and annealing temperatures, of the heavily cold worked metals. This rules out the possibility of employing a heavily cold worked material as a sample for thermal behaviour investigations.

The present work consists in suitably employing X-ray peak shift technique to evaluate the thermal behaviour of stacking faults in copper.

A sample with constant dislocation density at different temperatures is equivalent to a sample with different stacking fault parameters having the faults attained their equilibrium widths at those temperatures. The relative variation of the stacking fault parameter with respect to the one at room temperature can be obtained from the knowledge of the variation of peak shift relative to the peak positions at room temperature. From the knowledge of stacking fault energy at room temperature worked out by earlier workers, it is possible to work out the fractional variation of stacking fault

energy with respect to the room temperature value. In doing so, the variation of other parameters like lattice expansion and shear modulus with temperature are to be taken into account. Though none of the earlier works has taken into account the anisotropy of the lattice and the variation of anisotropic elastic constant with temperature, it would be interesting and more exact, if we could incorporate these factors also in our computations of stacking fault energy.

For an anisotropic f.c.c. lattice, the expression relating the stacking fault energy and fault width as worked out by Spence[33] is,

$$\gamma = K b_p^2 / 8\pi\eta \qquad \ldots\ldots(9)$$

$\vec{b}_p$ being the Burgers vector of partials and η, the separation of them. The anisotropic elastic coefficient K is given by

$$K = (K_e + K_s) - 2 (K_e - K_s) \cos 2\phi \qquad \ldots\ldots(10)$$

The angle 'ϕ' is subtended at the dislocation axis by the complete Berger's vector $\vec{b}_c = \vec{b}_{p1} + \vec{b}_{p2}$. The coefficients K_e and K_s are associated respectively with the edge and screw components of the partial Burger's vectors $\vec{b}_{p1}$ and $\vec{b}_{p2}$, and are functions of the elastic coefficients Cij of the crystal. The relations are given by:

$$K_s = \left[\frac{C^\circ_{44}}{2}\left(C^\circ_{11} - C^\circ_{12}\right)\right]^{\frac{1}{2}} \qquad \ldots\ldots(11)$$

$$\text{and} \quad K_e = \left(C^\circ_{11} + C^\circ_{12}\right)\left[\frac{C^\circ_{44}\left(C^\circ_{11} - C^\circ_{12}\right)}{C^\circ_{11}\left(C^\circ_{11} + C^\circ_{12} + 2C^\circ_{44}\right)}\right]^{\frac{1}{2}} \qquad \ldots\ldots(12)$$

The superscript zero on the Cij indicates the normal elastic constants referred to the crystal axes.

In the absence of suitable techniques to distinguish between edge and screw dislocations, it may not be too unreasonable to assume, that there are as many edge dislocations as there are of the screw type. Under such assumption, the value of K in the relation (10) becomes:

$$K = \left(K_e + K_s \right)$$

from relations (7) and (9) we get the relation between 'α' and 'γ' as

$$\gamma = \frac{K b_p^2 \rho d}{8\pi\alpha} = \text{Const.} \frac{K a^3}{\alpha} \qquad \ldots\ldots(13)$$

considering the ratio between the stacking fault energy value at any temperature and the value at room temperature,

$$\gamma_T / \gamma_{RT} = \left[K_T / K_{RT} \right] \left[\alpha_{RT} / \alpha_T \right] \left[\frac{a_T}{a_{RT}} \right]^3$$

The values of α_T can be obtained from the knowledge of the relative shift in the peak positions of any two selected peaks and employing the pattesons equation.

$U_T \alpha_T = (\Delta\Delta 2\theta)_T$, the various parameters having the same meaning as explained earlier.

Since the observed values of peak shifts at different temperatures are superimposed by the shifts introduced due to thermal expansion of the lattice, to get the shifts corresponding to the variation of stacking fault energy alone, the observed values should be corrected for contribution due to thermal expansion. It may be recalled here, that the effect of thermal expansion of the lattice is

to shift all peak positions towards the low 2θ values, while the direction of shift due to the variation of stacking fault energy is a function of the peak indices.

II EXPERIMENTAL TECHNIQUE

A) Preperation and mounting of the Sample

Polycrystalline Copper of 99.999% purity obtained in the form of rods from A.D. Mackay Incorporated N.Y., was machined to semi-cylindrical shape with cylindrical base so that it can conveniently be housed in the refractory pedastal, of the high temperature Camera; as shown in the figure (5).

The sample was sealed under Nitrogen gas in a Pyrex glass tube and was annealed for 50 minutes at 300°C in a muffle furnace in order to remove the faults introduced due to mechanical working.

The sample was mounted on the central refractory pedastal of the high temperature camera fitted on to the Diffractometer, so that the flat face of the specimen is exposed for X-rays. Provision for critical alignment is made through three independent motions translation, rotation and tilt which are completely independent of furnace proper.

B) Temperature Control:

Precise temperature control is made possible with the thermocouple activated magnetic amplifier system provided, and the continuously proportining saturable core reactor unit permits smooth, stepless control.

The heating chamber produces a zone of uniform temperature such that the sample face is maintained at less than $\pm$ 2°C at 500°C and less than $\pm$ 5°C at 1400°C.

The sample temperatures were recorded by a potentiometer using Platinum - 10% Rodium thermocouple. The accuracy of temperature measurement is estimated to be ± 1°C. Oxidation of the sample was prevented by continuous circulation of Nitrogen gas through the camera. The outcoming gas was bubbled through oil to ensure continuous flow without leakage in the set up.

C) Intensity measurements

The line profiles of (111) and (200) reflections were recorded at temperatures of 300°K, 393°K, 470.5°K, 528.0°K, 623.0°K and 727°K (± 1°K) with a General Electric proportional counter diffractometer equipped with X RD-6 X-ray generator and SPG - 4 detector, using Ni-filtered Cu - $K\alpha_{\phi}$ radiation.

The line shapes were recorded manually and measurements were made of the diffracted intensity by point counting at intervals in 2Θ varying from 0.1° in the general background to 0.01° near the maxima of the peaks, where Θ is the Bragg angle.

To minimise the positioning errors, the measurements of both the peaks at each temperature were carried out in a single and continuous run.

A beam slit of 3° with 0.1° detector was employed throughout the measurements. The point counting of intensity was done by employing a proportional counter using a time constant of one minute.

The time taken for scanning the two peaks varied from 30 to 45 minutes while the variation of the temperature of the furnace during this period was of the order ± 1.5°C.

III RESULTS AND DISCUSSION

Seperation of α_1 from doublet and calculating peak positions

From the knowledge of the point counts, the line profiles of the peaks were graphically plotted. Rachingers[34] method (given in the appendix) was employed to seperate the α_1 peak from the doublet.

The point of maximum intensity cannot be taken as the position for peak maximum due to statistical fluctuations.

Several methods have been proposed for obtaining the peak positions graphically but each of them suffers from its own disadvantage and was subjected to criticism. However, in the present work the peak positions of (111) and (200) reflections were obtained by taking the mid - points of section lines drawn parallel to the background level and extrapolating to the peak maximum as was done by several authors[35,36] recently. The method is illustrated in the appendix. The accuracy in the determination of peak positions is estimated to be 0.05° in 2θ value. Since the effect of thermal expansion of the lattice is to shift all reflections to low 2θ value, the observed peak positions were corrected by adding the shift contribution in 2θ value due to the rise in temperature[37] and the values are given in table (2).

Computation of Peak Shifts

On the assumption that the peak shift equivalent due to Stacking Fault Energy at room Temperature is 0.09° (in 2θ) as obtained by Wagner[22] for 99.999% Pure Copper, the relative peak shifts at various temperatures were computed.

These results giving details of lattice parameter, observed

peak positions, corrected peak positions and relative peak shifts at various temperatures are tabulated in table (3). The ratio of Stacking fault energy at any temperature to the one at room temperature is

$$\frac{\gamma_T}{\gamma_{RT}} = \left[\frac{K_T}{K_{RT}}\right]\left[\frac{\alpha_{RT}}{\alpha_T}\right]\left[\frac{a_T}{a_{RT}}\right]^3$$

The effective elastic constant K is related to the elastic coefficients C_{ij} as

$$K = K_\epsilon + K_s = (C_{11}^\circ + C_{12}^\circ)\left[\frac{C_{44}^\circ (C_{11}^\circ - C_{12}^\circ)}{C_{11}^\circ (C_{11}^\circ + C_{12}^\circ + 2C_{44}^\circ)}\right]^{\frac{1}{2}} + \left[\frac{C_{44}^\circ}{2}(C_{11}^\circ - C_{12}^\circ)\right]^{\frac{1}{2}}$$

The values of elastic constants C_{44}°, C_{11}° and C_{22}° measured for 99.999% pure Copper over the temperature range 300°K to about 800°K using the Conventional Ultrosonic Pulse-echo technique, were reported recently by Y.A. Chang and L. Himmel[36]. Using these values, the effective elastic constant 'K' was calculated at various temperatures and is given in table No. (1). The values of the stacking fault probabilities at various temperatures have been arrived at by employing the Pattersons equation.

$$\Delta\Delta 2\theta_T = H\alpha_T$$

The values of stacking fault parameter 'α', effective elastic constant 'K' and the ratio of S.F.E at any temperature to the one at room temperature, are given in Table (4). It can be seen that the general tendency is that the ratio $\left(\frac{\gamma_T}{\gamma_{RT}}\right)$ is decreasing with temperature, similar to the nature of variation reported for Silver.[30,31]

A best fit Straight line has been computed by least square method and the general law of variation was,

found to be $\frac{\gamma_T}{\gamma_{RT}} = 1.2377 - .000827\ T$

where γ_T is the stacking fault energy at any temperature T° K, γ_{RT} is the SFE at room temperature.

An intrinsic stacking fault in a f.c.c crystal can be regarded as two close packed planes of a hcc.p phase, and a stacking fault in h.c.p. as two close packed planes of a f.c.c phase. In a first approximation SFE per mole of stacking fault should then be equal to the difference in molar free energy between the f.c.c and h.c.p phases.

The nature of variation of molar free energies of f.c.c and h.c.p phases with temperature should govern the thermal behaviour of Stacking fault energy.

As is seen from table (4) the variation of $\left[\frac{\gamma_T}{\gamma_{RT}}\right]$ is from 1 to .607 in the temperature interval 300°K to 727°K. This would mean a decrease of S.F.E from 67[37] ergs/cm^2 to about 40.2 ergs/cm^2 in the observed temperature range.

The consequence of this variation of S.F.E with temperature is of considerable importance.

Since the extended dislocation with the enclosed Stacking Fault takes part as a unit in the climb or the cross slip process, the variation of the stacking fault width with temperature should govern the temperature dependence of strength, ductility, recovery recrystalisation and texture orientation.

In principle, lowering of stacking fault energy hinders the softening process involving cross slip because of increase in equilibrium width.

But this is true only when the property of the material is a function of stacking fault width alone and not influenced by temperature. Since most of the mechanical properties have a direct dependence on temperature itself. apart from the dependence on stacking fault width, much cannot be directly concluded regarding the temperature dependence of property of the material from the knowledge of thermal behaviour of stacking faults alone.

The absolute magnitudes of SFE worked out for a metal by various methods differ by so much in magnitude, that we can probably say that the present methods of measurement or based on less well founded basis. In such cases, it would be more meaningful to talk about the thermal variation of fractional S.F. E parameter γ_T/γ_{RT} which is the ratio of S.F.E at any temperature to the one at room temperature.

As pointed out by Klein[38], the method of employing cold worked filings cannot be relied upon here since the relating constant between S.F.E and stacking fault probability is strongly dependent on dislocation configuration which in turn is a function of annealing cycle.

To this extent, the present method claims more reliable results since by employing an annealed sample, the variation in the dislocation configuration can be ignored.

LIMITATIONS ON THE EXPERIMENTAL TECHNIQUE

The present experimental method suffers mainly from two disadvantages.

The reduced intensities resulting from severe monochromatization as well as limitation on the size and form of the sample result in prohibitively long experimental runs.

The statistical factors influencing the peak positions are:

a) size of counting step

b) sharpness of profile

c) signal to background ratio

d) counting rate

The accuracy of a given peak maximum determination in terms of these statistical factors is not known.

CONCLUSIONS

1. The patterson's theory which relates the stacking fault probability to the shift in peak maxima can conveniently be adopted to obtain a qualitative variation of S.F.E. with temperature.

   In doing so, correction for the thermal effects on elastic constant and lattice expansion should properly be incorporated.

2. Stacking Fault Energy was found to be linierly decreasing with temperature, the Law of variation being ,

$$\frac{\gamma_T}{\gamma_{RT}} = 1.2377 - 0.000827\ T$$

where γ_T is the Stacking Fault Energy at temperature T° K and γ_{RT} is the Stacking Fault Energy at room temperature.

R E F E R E N C E S

1. F.C. Frank, Phil. Mag. 42, 809 (1951)

2. R.D. Heidenreich and W. Shockley, Report on Strength of Solids (London Physical Society) 57, (1948)

3. F.C. Thompson and W. E. W. Millington, J. Iron and Steel Inst. 109, 67 (1924)

4. H, Hu, R.S. Cline and S.R. Goodman, Trans. AIME 224, 96, (1962)

5. N. Brown, Trans. AIME 221, 236 (1961)

6. H. Hu, R.S. Cline, J. Appl. Phy. 32, 760 (1961)

7. H. Hu, R.S. Cline, and S.R. Goodman, J. Appl. Phys. 32, 1392 (1961)

8. M.J. Whelan, P.B. Hirsh, R. W. Horne and W. Bollmann, Proc. Roy. Soc. (Lond.) A240, 524 (1957)

9. N.F. Mott, Trans. AIME 218, 962 (1960)

10. A. Seeger, Defects in Crystalline Solids, Bristol Conference; The Physical Soc. (Lond.) 1955, p. 328

11. A. Seeger, Dislocations and mechanical properties of crystals (John Wiley & Sons Inc. New York, 1956) p. 243.

12. P.R. Thronton and P.B. Hirsh, Phil. Mag. 3, 738 (1958)

13. M.J. Wielan, Proc. Roy. Soc. (London) A 249, 114 (1959)

14. A. Howie and P.R. Swann, Phil. Mag. 6, 1215 (1961)

15. C.N.J. Wagner, Acta. Met. 5, 427 (1957)

16. B.E. Warren, Progress in metal physics, Pergamon Press, N.Y. 1959, Vol. 8, p. 147

17. Willis, B.T.M. (1959) Acta. Cryst. 12, 683 p.

18. Warren, B. E. (1959) Progr. Metal Phys. 8, 147

19. M.S. Patter, J. Appl. Phys. 23, 805 (1952)

20. C.N.J. Wagner, A.S. Tetelman and H.M. Otte, J. Appl. Phys. 33, 3080 (1962)

21. C.S. Barret, Imperfections in nearly perfect crystals, Wiley, New York (1952)

22. C.N.J. Wagner, Acha. Met. 5, 427, Aug. 1957

23. R.G. Davies and R. W. Cahn, Acta Met. 10, 621 (1962)

24. F.H. Foley, R.W. Cahn and G.V. Rayor, Acta Met. 11, 355 (1963)

25. L.F. Vassamillet, J. Appl. Phys. 32, 778 (1961)

26. L.F. Vassamillet and T.B. Massalski, J. Appl. Phys. 35, 2629 (1964)

27. Christian, J.W. and Spreadborough, J., Phil. Mag. 8, 1069 (1956)

28. Warren, B.E. and Warekois, E.P., Acta Met. 3, 473 (1956)

29. P. Swann and J. Nutting, J. Inst. Metals 90, 133 (1961, 62)

30. S.E. Buhler, K. Lucke and F.W. Rosenbaum, Phys. Status Solidi 3,886 (1963)

31. Schwab S. Major, J. Appl. Phys. 37, 4275 (1966)

32. Mark J. Klein, Scripta Met. 1, p.66 (1967)

33. G.B. Spence, J. Appl. Phys. 33, 729 (1962)

34. W.A. Rachinger, J. Sci. Instr. 25, 254 (1948)

35. K.N. Goswami, S.P. Sen Gupta, Acta. Met. 14, 1559, 1966

36a. S.P. Sen Gupta and M.A. Quader, Acta Crystallogs (In press) (Ref. 15 in 35)

36b. Y.A. Chang and L. Himmel, J. Appl. Phy. Vol. 37, No. 9, Aug.1966 p. 3567

37. Handbook of lattice spacings by "Pearson"

38. H.M. Otte, J. Appl. Phys. 38, p. 217, 1967

39. Mark J. Klein, Scripta Met. Vol. 1, 65, 1967

- oOo -

VARIATION OF ANISOTROPIC ELASTIC CONSTANT WITH TEMPERATURE

```
C  C     RAO     MTG 022
       DO 5 I1,6
       READ,T,C11,C12,C44
       AK=(C44*(C11-C12))**(0.5)
       AKS=AK/(2.**.5)
       AKE=(3*C11-C12)*AK/(C11*(C11+C12+C44*2.)**0.5)
       CAL=AKE+AKS
       CAL=2.*(AKE-AKS)
   10  FORMAT (1X,F6.1,2F8.4)
    5  CONTINUE
       STOP
       END
         300., 1.700, 1.225, 0.750
         393., 1.650, 1.200, 0.733
         470.5, 1.628, 1.191, 0.712
         528., 1.609, 1.17?, 0.677
         673., 1.566, 1.109, 0.671
           727., 1.49, 1.14?, 0.669
```

TABLE: I

```
C  C     RAO     MTG 022
```

T^0_K	(K_e+K_s) $\times 10^{12}$ dynes/cm^2	$2(K_e-K_s)$ $\times 10^{12}$ dynes/cm^2
300.0	.9142	.1312
393.0	.8848	.1410
470.5	.8655	.1490
528.0	.8409	.1544
673.0	.8195	.1620
727.0	.7813	.1726

```
C  C     RAO     MTG 022
       DIMENSION DP(6),DD(6),DP1(6),DP2(6),P1(6),P2(6)
       DO 5 I=1,6
       READ,T,A
       D1=(2.5418*1.002*(3.**.5))/(2.*A)
       D2=(2.5418*2.004)/(2.*A)
       P1(I)=2.*((ATAN(D1/((1.-D1**2)**.5)))*(180./(3.*ATAN(1.))))
       P2(I)=2.*((ATAN(D2/((1.-D2**2)**.5)))*(180./(3.*ATAN(1.))))
       DP(I)=P1(I)-P2(I)
       DP1(I)=P1(I)-P1(1)
       DP2(I)=P2(I)-P2(1)
       DD(I)=DP(I)-DP(1)
10     FORMAT (1X,F6.1,7F9.4)
5      PUNCH 10,T,A,P1(I),DP1(I),P2(I),DP2(I),DP(I),DD(I)
       STOP
       END
       300.,3.6080
       393.,3.6141
       473.,3.6182
       528.,3.6230
       623.,3.6294
       727.,3.6366
```

Table: II

```
C  C     RAO     MTG 022
```

$T^\circ K$	a_T Å	$(2\theta^\circ_{111})_T$	$(\Delta 2\theta^\circ_{111})_T$	$(2\theta^\circ_{200})_T$	$(\Delta 2\theta^\circ_{200})_T$	$\Delta 2\theta^\circ$ $(2\theta_{111}-2\theta_{200})$	$\Delta\Delta 2\theta^\circ$ $(\Delta 2\theta_T-\Delta 2\theta_{300^\circ K})$
300.0	3.6080	37.6855	0.0000	44.9022	0.0000	-7.2168	0.0000
393.0	3.6141	37.6106	-.0747	44.8059	-.0963	-7.1951	.0216
473.0	3.6182	37.5608	-.1247	44.7415	-.1607	-7.1807	.0361
528.0	3.6230	37.5024	-.1830	44.6663	-.2359	-7.1659	.0509
623.0	3.6294	37.4250	-.2605	44.5665	-.3357	-7.1416	.0752
727.0	3.6366	37.3382	-.3473	44.4549	-.4473	-7.1167	.1001

```
0      STOP  END OF PROGRAM AT  STATEMENT 0005 + 01 LINES
```

TABLE 3

T_K°	$2\theta_{111}$ observed	$\Delta 2\theta_{111}$ Lattice expn Correction	$2\theta_{111}$ Due to faults alone	$2\theta_{200}$ Observed	$\Delta 2\theta_{200}$ Lattice expn correction	$2\theta_{200}$ Due to faults alone	$(2\theta_{200} - 2\theta_{111})$ $\Delta 2\theta_T$	$\Delta\Delta 2\theta$ $(\Delta 2\theta_T - \Delta 2\theta_{RT})$	$(\Delta\Delta 2\theta + .09)$
300.0	42.65	0.0000	42.6500	49.81	0.0000	49.8100	7.1600	0.0000	0.0900
393.0	42.63	0.0747	42.7047	49.78	0.0963	49.8763	7.1716	0.0116	0.1016
476.5	42.58	0.1247	42.7047	49.78	0.1007	49.8807	7.1760	0.0160	0.1060
526.0	42.62	0.1030	42.7030	49.83	0.2359	49.8659	7.1629	0.0029	0.0929
623.0	42.41	0.2605	42.6705	49.82	0.3357	49.8557	7.1857	0.0257	0.1157
727.0	42.33	0.3473	42.6973	49.45	0.4473	49.8973	7.2000	0.0400	0.1300

TABLE 4

```
MTG 022  RAO
      DIMENSION GAMA(6), FGAMA(6)
      DO 5 I=1,6
      READ,T,C,A,DDPHI,PHI1,PHI2
      PHI1=PHI1*(4.*ATAN(1.)/180.)
      PHI2=PHI2*(4.*ATAN(1.)/180.)
      H=(7.9*(SIN(PHI1)/COS(PHI1))+3.95*(SIN(PHI2)/COS(PHI2)))
      ALPHA=DDPHI/H
      GAMA(I)=UC*(A**3.))/ALPHA
      FGAMA(I)=GAMA(I)/GAMA(1)
      FORMAT (1X,F5.1,4F9.4,F15.4,F9.4)
      PUNCH 10,T,A,C,H,ALPHA,GAMA(I),FGAMA(I)
      STOP
      END
300.0,0.9142,3.6080,0.0900,24.9050,21.3250
393.0,0.8848,3.6141,0.1016,24.9381,21.3523
470.0,0.8633,3.6182,0.1060,24.9303,21.3423
528.0,0.8469,3.6230,0.0929,24.9329,21.3513
623.0,0.8195,3.6294,0.1152,24.9278,21.3352
7_7.0,0.7813,3.6366,0.1300,24.9486,21.3486
```

°K	a_T Å	$K \times 10^{-12}$ dynes/cm² (K_e+K_s)	H	α	const (γ_T)	γ_T/γ_{RT}*
0	3.6080	.9142	3.2099	.0173	2485.5917	1.0000
0	3.6141	.8848	3.2176	.0193	2144.9955	.8630
5	3.6182	.8633	3.2135	.0203	2012.0233	.8095
0	3.6230	.8469	3.2107	.0176	2261.6111	.9099
0	3.6294	.8195	3.2146	.0221	1773.4478	.7135
0	3.6366	.7813	3.2191	.0249	1508.5427	.6069

```
 STOP  END OF PROGRAM AT  STATEMENT 0005 + 01 LINES
```

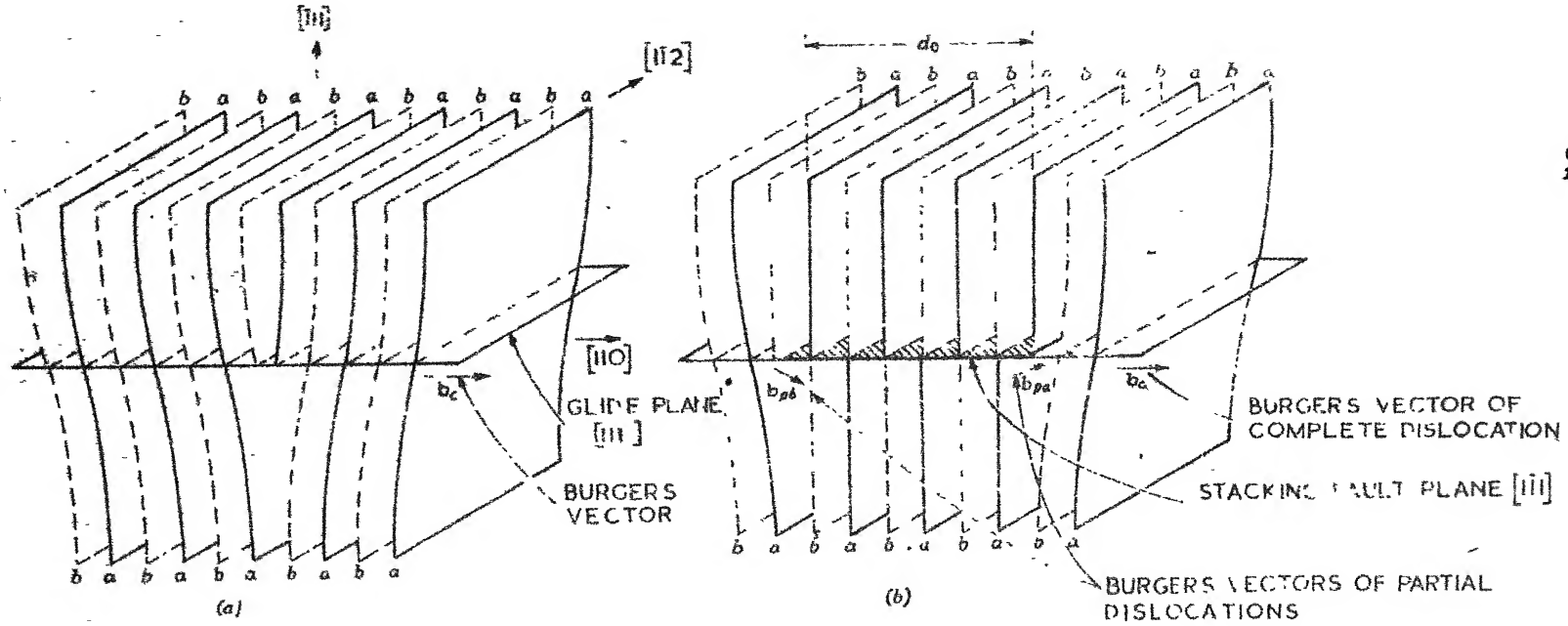

FIG. [1] EDGE DISLOCATION IN THE FACE-CENTERED CUBIC LATTICE (a) UNEXTENDED DISLOCATION (b) EXTENDED DISLOCATION WITH $\eta = 3b$

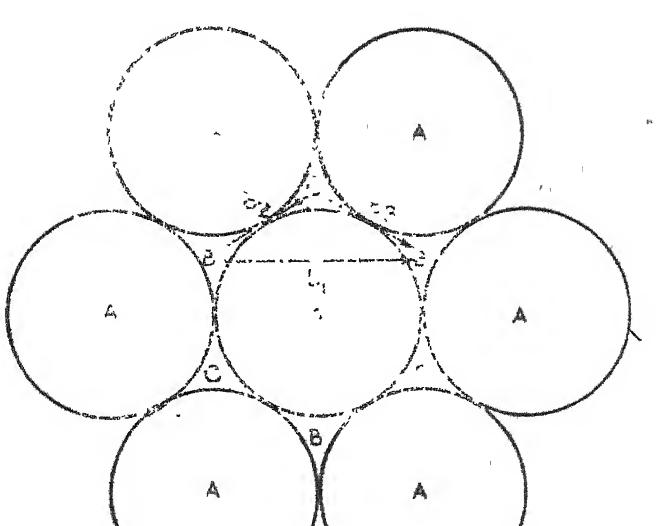

FIG. [2] VECTOR DIAGRAM INDICATING THE ATOMIC MOTIONS RESULTING IN SLIP (FROM COTTRELL, DISLOCATIONS AND PLASTIC FLOW IN CRYSTALS, CLARENDON PRESS, OXFORD, 1953)

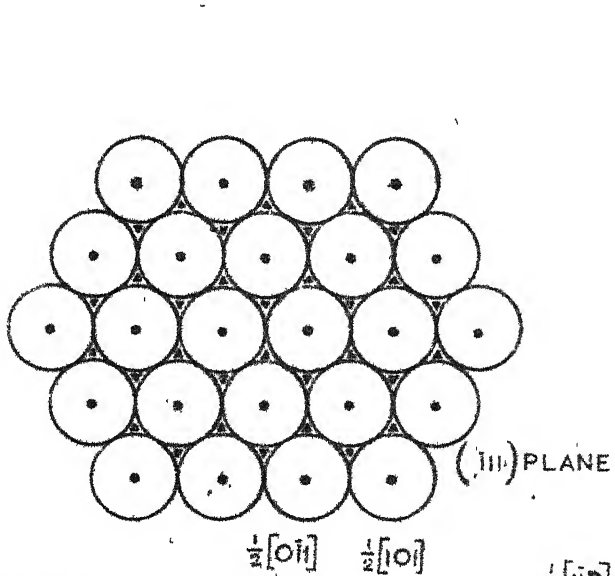

FIG. [3] A CLOSE-PACKED (111) PLANE OF A FACE-CENTERED CUBIC LATTICE. THE MARKINGS A,B,C INDICATE THE PROJECTIONS OF THE POSITIONS OF THE CENTERS OF SPHERES IN A,B,C LAYERS. THE PATTERN IS THE SAME IN THE BASAL OF THE HEXAGONAL CLOSE PACKED STRUCTURE. THE CRYSTALLOGRAPHIC NOTATIONS IN FIG. [3] HOWEVER, REFER TO THE FACE CENTERED CUBIC LATTICE.

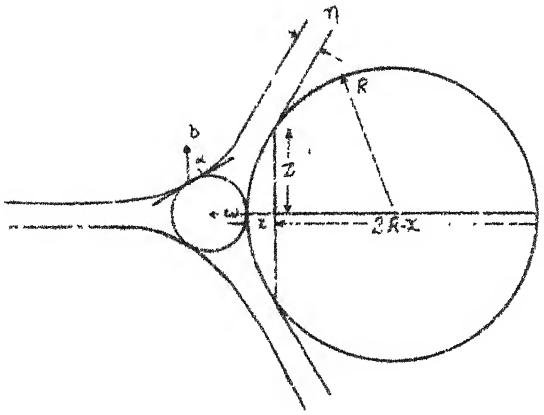

EXTENDED NODE

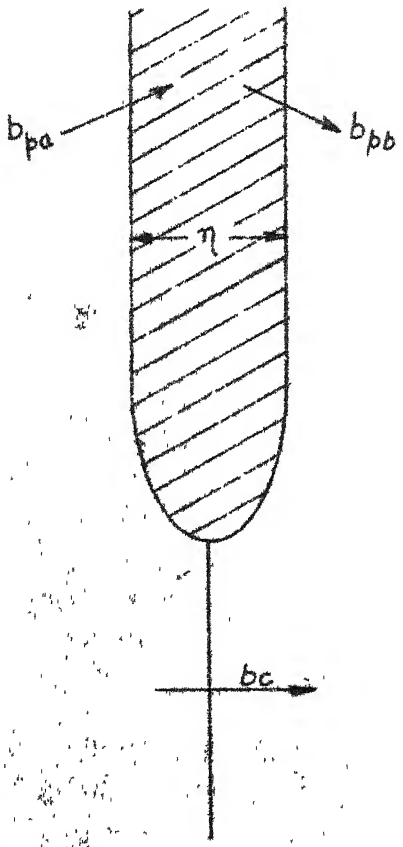

EXTENDED DISLOCATION

FIG. [A1]

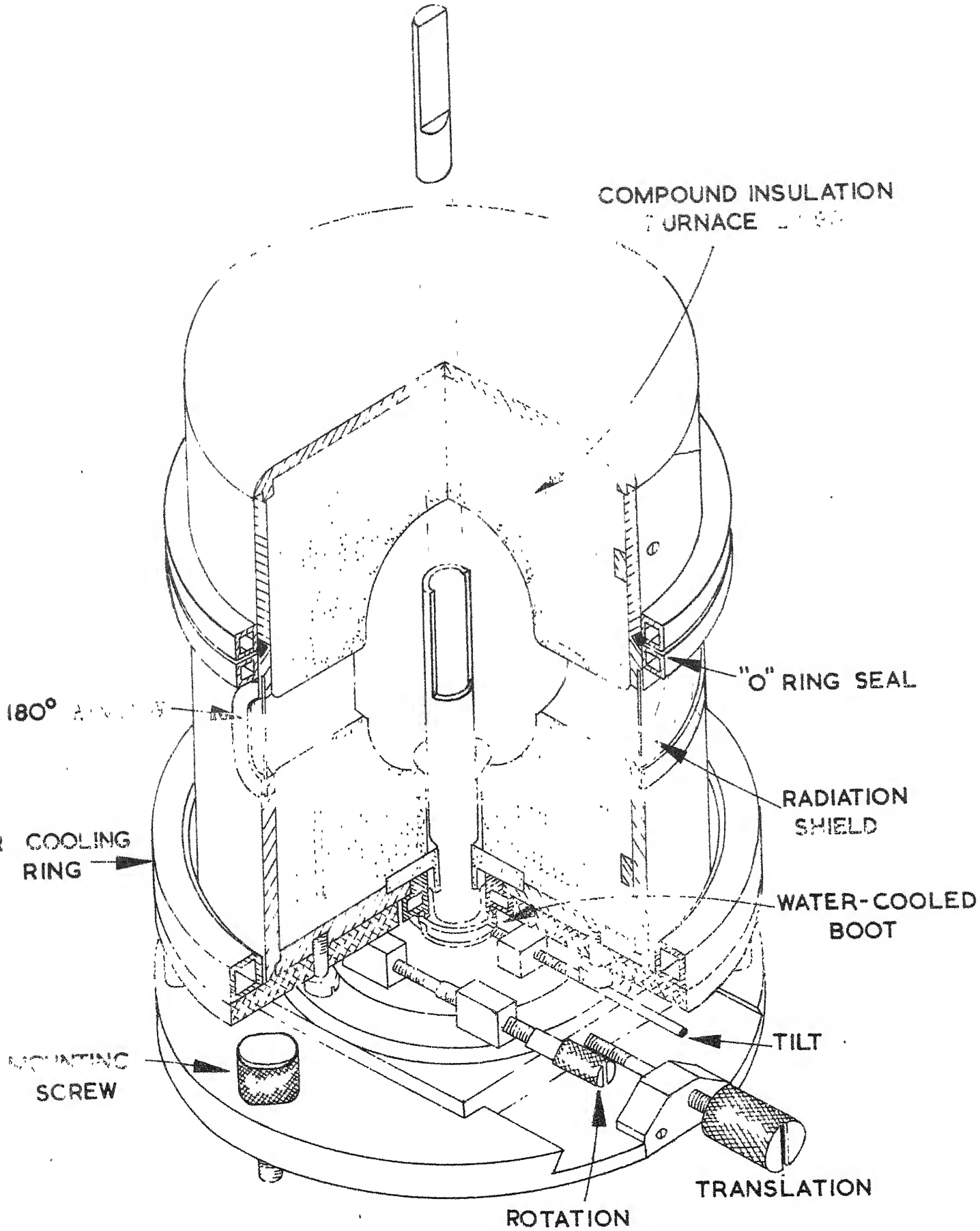

TEM-PRES HIGH TEMPERATURE
X-RAY DIFFRACTOMETER FURNACE.
FIGURE. [5].

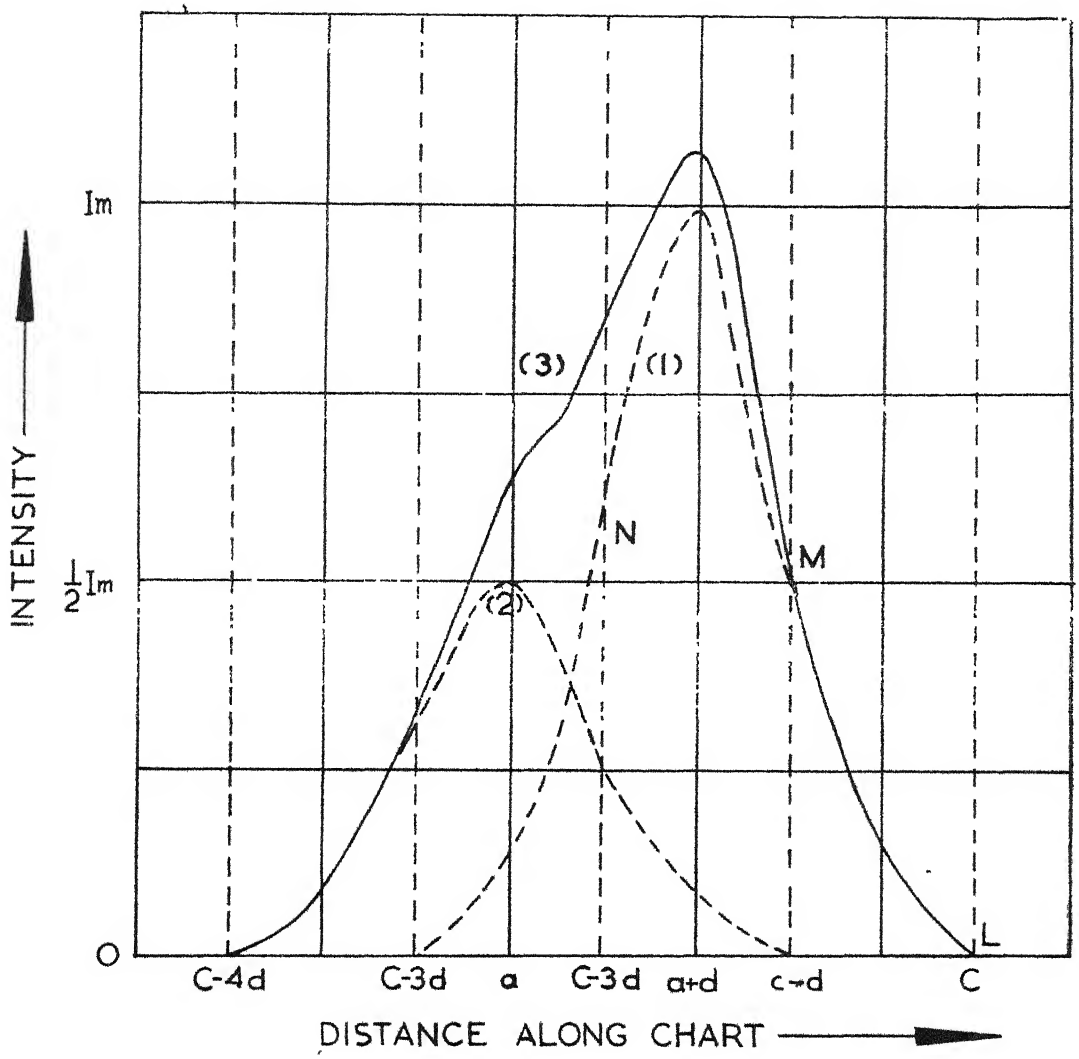
Im
½Im
O
INTENSITY
(3)
(1)
(2)
N
M
L
C-4d
C-3d
a
C-3d
a+d
c+d
C
DISTANCE ALONG CHART

Fig [6]

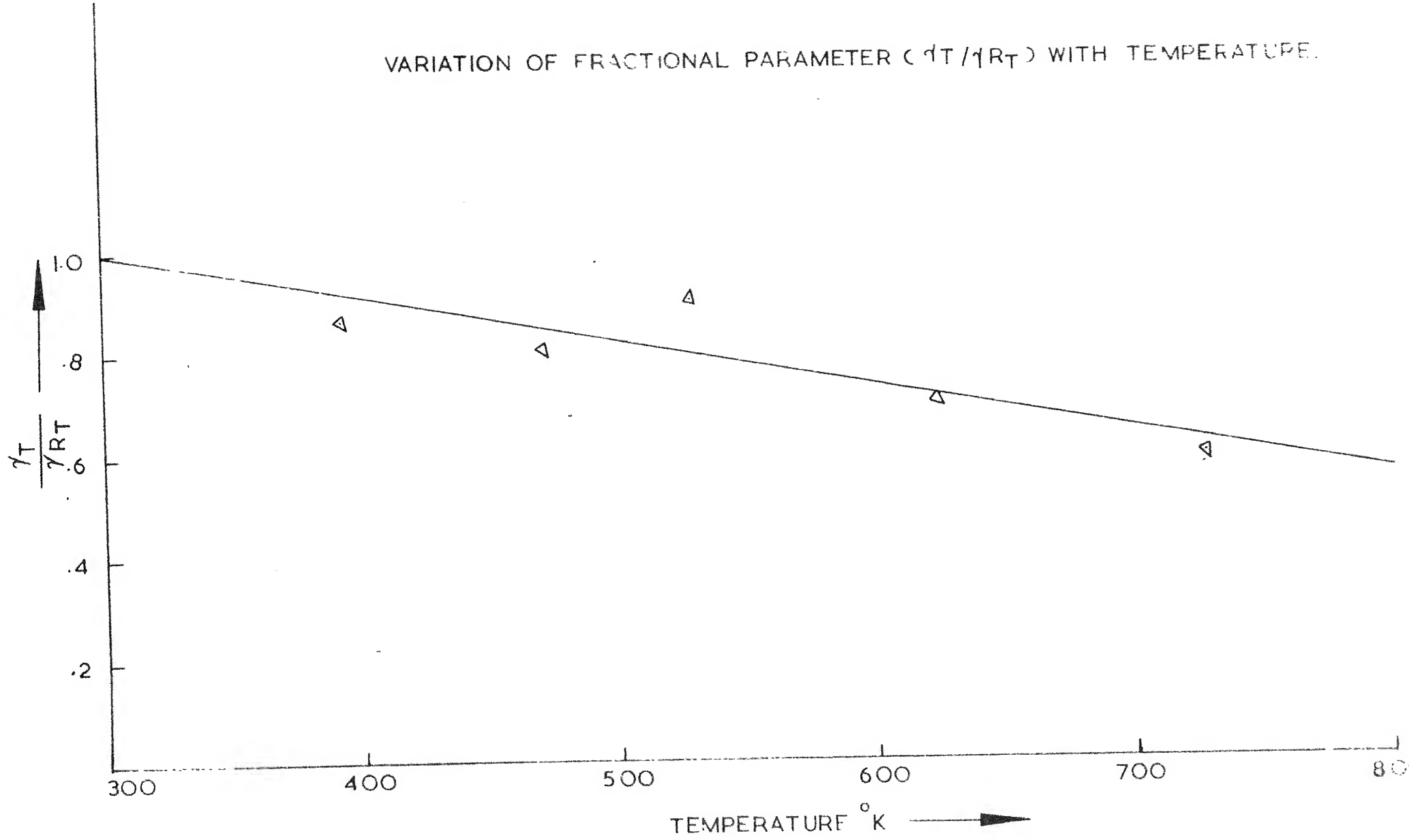
VARIATION OF FRACTIONAL PARAMETER (γT / γRT) WITH TEMPERATURE.
γT / γRT
1.0
.8
.6
.4
.2
300
400
500
600
700
800
TEMPERATURE °K

Fig(7)

APPENDIX

A CORRECTION FOR THE $\alpha_1 \alpha_2$ DOUBLET IN THE MEASUREMENT OF WIDTHS OF X-RAY DIFFRACTION LINES AND LOCATING THE PEAK MAXIMUM OF COMPONENT

In studies of particle size, lattice distortion and stacking fault effects in crystalline materials by the measurement of X-ray diffraction line widths, an inherent difficulty is due to the doublet structure of the lines. These doublet components overlap when the line becomes broadened and the problem is to obtain the width of the stronger α_1 component in the presence of the α_2.

The only date available for the measurement of the width of the single line are :

(a) the intensity trace of the composite line ($\alpha_1 + \alpha_2$);

(b) the separation of the doublet components which can be calculated from the spacing of the reflecting plane, the α_1 and α_2 wave-lengths, and the geometry of the apparatus;

(c) the ratio of intensity of α_1 to that of α_2, which has been determined by various workers and may be taken as 2.

The position is illustrated in the accompanying figure in which is shown a plot of intensity (I) against film distance (x) for the α_1 and α_2 components of the diffraction line and their resultant sum $\alpha_1 + \alpha_2$ the latter being the idealized photometer trace of the line.

The α_1 and α_2 components may be represented respectively by the equations :

$$I_{\alpha_1} = f (x - d), \qquad (1)$$

$$I_{\alpha_2} = \tfrac{1}{2} f (x) \qquad (2)$$

where d is the doublet separation.

The factor of one-half in equation (2) is a consequence of the fact that

(Intensity of α_1 component)/(Intensity of α_2 component) = 2

The peak intensity of the α_1 component is

$$I_m = f (a).$$

The procedure is based on the following observation. It is obvious from equations (1) and (2) that if the intensity of the α_1 component becomes effectively zero at x = c then the α_2 curve falls to zero at x = c - d. Thus the resultant $\alpha_1 + \alpha_2$ curve will be coincident with the α_1 curve LM throughout the range $c - d \leq x \leq c$. Then from this known part of the α_1 curve one can deduce the remaining shapes of the α_1 and α_2 component curves.

The first step is as follows : Divide the graph into rectangular strips by ordinates whose seperation is d, the first ordinate being the line x = c. These ordinates are shown dotted in the figure. The curve in the range $c - 2d \leq x \leq c - d$ can be constructed from the section of the photometer trace included between the lines x = c - d and x = c (i.e. the curve LM) by reduction of the ordinates of LM by the factor of one-half and a translation of this curve through a distance of d in the (- x) direction. Then the α_1 curve in this range (MN) is obtained by subtraction of the α_2 curve from the composite ($\alpha_1 + \alpha_2$) (i.e. the microphotometer trace).

The procedure is then repeated, the α_2 curve in the range $c - 3d \leq x \leq c - 2d$ being obtained by halving the ordinates of the α_1 curve MN and displacing this reduced curve a distance (-d). The α_1 curve in this range is then obtained by subtraction and the process is again repeated until the curve is completely resolved. This construction of the α_2 curve from that of the α_1 by reduction of the α_1 ordinates by one-half, followed by a translation of the reduced curve through a distance -d, is easily carried out using a parallel sided rule of width d (the doublet separation). The right-hand edge of the rule is laid parallel to the I axis intersecting the α_1 curve at a height 'h' above the 'x' axis. The corresponding point of the α_2 curve is then located on the left-hand edge of the rule at a height (1/2 h) above the x axis.

To find the peak maxima of the α_1 component, section lines are drawn parallel to the back-ground level and the mid points of these section lines are located. The extrapolation of these mid-points of the section lines drawn parallel to the back-ground level gives the peak maximum position as shown in Figure (7).